



## Amplification and Spread of Viruses in a Growing Plaque

LINGCHONG YOU AND JOHN YIN\*

*Department of Chemical Engineering, University of Wisconsin-Madison,  
1415 Engineering Drive, Madison WI 53706-1691, U.S.A.*

*(Received on 3 August 1998, Accepted in revised form on 9 July 1999)*

The two-dimensional propagation of viruses through a “lawn” of receptive hosts, commonly called plaque growth, reflects the dynamics of interactions between viruses and host cells. Here we treat the amplification of viruses during plaque growth as a reaction–diffusion system, where interactions among the virus, uninfected host cells, and virus-producing host–virus complexes are accounted for using rates of viral adsorption to and desorption from the host–cell surface, rates of reproduction and release of progeny viruses by lysis of the host, and by the coupling of these reactions with diffusion of free virus within the agar support. Numerical solution of the system shows the development of a traveling wave of reproducing viruses, where the velocity of the wave is governed by the kinetic and diffusion parameters. The model has been applied to predict the propagation velocity of a bacteriophage plaque. Different mechanisms may account for the dependence of this velocity on the host density during early stages of a growing plaque. The model provides a means to explore how changes in the virus–host interactions may be manifest in a growing plaque.

© 1999 Academic Press

### Introduction

A plaque is a region of lysed host cells, visible to the naked eye, and formed by the growth of viruses in a thin layer of hardened agar containing evenly distributed host cells. Plaque growth starts when a free virus particle diffuses to a host cell, adsorbs to its surface, replicates within, and finally lyses it, releasing a new generation of infective viruses, which in turn diffuse to neighboring hosts and repeat the progress. Plaques are useful. The titer of infective virus particles in a liquid sample can be measured by mixing it with receptive hosts in agar, pouring the mixture into a Petri dish, allowing the agar to gel, incubating

for several hours, and then counting the visible plaques formed. Moreover, the size, shape, and clarity or turbidity of plaques have historically been used to characterize different virus strains. Finally, since plaques are initiated by a single virus particle and a single plaque easily produces a million virus descendants, “plaque purification” is a standard means for generating a relatively homogeneous sample of a particular virus strain (Sambrook *et al.*, 1989).

Using phage T7 growing on *E. coli* as a model system, we discovered in a single plaque that mutant phage strains can appear and outgrow their precursor, sometimes forming uneven bulged regions along the plaque boundary, where their propagation is presumably enhanced (Yin, 1993, 1994; Lee & Yin, 1996a). Within a growing plaque, viruses only compete locally

\* Author to whom correspondence should be addressed.  
E-mail: [yin@engr.wisc.edu](mailto:yin@engr.wisc.edu)

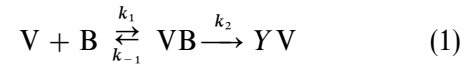
for host resources; fast-growing mutant strains only influence the composition of virus populations along the sector where they arise. Hence, the propagation and genetic diversification of viruses during plaque growth can sustain a potentially broader distribution of mutants than well-mixed virus cultures. To complement our laboratory studies, it is important to understand the relationship between the propagation velocity, a key phenotype of the virus–host interaction, and the dynamic properties of the system. These include contributions from viral diffusion, viral adsorption to the host, the latent or generation time, the yield of viral progeny per infected host, and the effect of host growth on these processes.

More than three decades ago, Koch (1964) described the growth of viral plaques during the enlargement phase, studying phage T4 growing on *E. coli* as a model system. Using heuristic arguments he suggested that  $c = a(D/L)^{1/2}$ , where  $c$  is the radial propagation velocity of the expanding plaque,  $D$  is the viral diffusivity through the mixed medium,  $L$  is the latent time for viral replication in infected host and  $a$  is a constant. Koch modified this equation for cases of reversible and irreversible viral binding to the host, effects that are embedded in the constant  $a$ . More recently, we set up a reaction–diffusion model for plaque growth that explicitly took account of the reversible binding of virus to the host cell (Yin & McCaskill, 1992). By assuming the existence of a traveling-wave solution, we were able to obtain an implicit expression for the propagation velocity in terms of the reaction parameters of the system and the viral diffusivity through the mixed media. For several limiting cases, explicit expressions for the propagation velocity were derived, but due to the sparseness of relevant kinetic data, none of these cases was clearly more relevant than the others.

In this study, we use numerical methods to solve the full reaction–diffusion model and investigate the effect of various model parameters on the propagation velocity. In contrast to our earlier work, we make no *a priori* assumption here about the form of the solution. Instead, the simulation reveals the existence of a traveling wave for the system.

### Mathematical Model

We model the plaque growth process by considering the interactions among three species: the free virus particle (V), the uninfected host bacteria (B), and virus–host cell complex (VB). The reactions involved may be summarized as follows:



where  $Y$  is the yield of new virus particles per lysed host cell,  $k_1$ ,  $k_{-1}$ , are adsorption and desorption rate parameters, respectively, and  $k_2$  is inversely proportional to the latent time of intracellular virus growth. We assume that free virus particles diffuse through the mixed medium formed by the agar and embedded hosts, while both infected and uninfected host cells are immobilized. Plaque boundaries are circular, so we work in polar coordinates and write down the rate equations for all the species as functions of position ( $r$ ) and time ( $t$ ):

$$\begin{aligned} \frac{\partial[V]}{\partial t} = D_{eff} \left( \frac{\partial^2[V]}{\partial r^2} + \frac{1}{r} \frac{\partial[V]}{\partial r} \right) - k_1[V][B] \\ + (k_{-1} + Yk_2)[VB] \end{aligned} \quad (2a)$$

$$\frac{\partial[B]}{\partial t} = -k_1[V][B] + k_{-1}[VB] \quad (2b)$$

$$\begin{aligned} \frac{\partial[VB]}{\partial t} = k_1[V][B] \\ - k_{-1}[VB] - k_2[VB] \end{aligned} \quad (2c)$$

with

BC:

$$[V] = 0, \quad [VB] = 0 \quad \text{as } r \rightarrow \infty,$$

$$\frac{\partial[V]}{\partial r} = 0 \quad \text{at } r = 0 \text{ and } r \rightarrow \infty.$$

IC:

$$[V] = \begin{cases} V_0 & r \leq r_0 \\ 0 & r > r_0 \end{cases} \quad \text{at } t = 0,$$

$$[B] = \begin{cases} 0 & r \leq r_0 \\ B_0 & r > r_0 \end{cases} \text{ at } t = 0,$$

$$[VB] = 0, \text{ at } t = 0 \text{ for all values of } r,$$

where  $D_{eff}$  is the effective virus diffusivity, defined as  $Dg(\phi)$ .  $D$  is the diffusion constant of virus through agar in the absence of hosts,  $\phi$  is the volume fraction of the host cells in the medium, and  $g(\phi)$  is a function of  $\phi$  that ranges from 1 to 0 as  $\phi$  ranges from 0 to 1; unlysed host cells may act as a barrier to virus diffusion. We employ a volume fraction in a two-dimensional (2D) model, assuming components normal to the plane of the plaque are uniform. The effect of host cells on viral diffusion can be neglected by setting  $g(\phi)$  to 1.

We cast the original equations into dimensionless form by introducing  $V = [V]/B_0$ ,  $B = [B]/B_0$ ,  $I = [VB]/B_0$ ,  $\tau = k_2t$ ,  $x = (k_2/D)^{1/2}r$ ,  $\kappa_1 = k_1B_0/k_2$  and  $\kappa_{-1} = k_{-1}/k_2$ :

$$\frac{\partial V}{\partial \tau} = g(\phi) \left( \frac{\partial^2 V}{\partial x^2} + \frac{1}{x} \frac{\partial V}{\partial x} \right) - \kappa_1 VB + (\kappa_{-1} + Y)I, \tag{3a}$$

$$\frac{\partial B}{\partial \tau} = -\kappa_1 VB + \kappa_{-1}I, \tag{3b}$$

$$\frac{\partial I}{\partial \tau} = \kappa_1 VB - (\kappa_{-1} + 1)I, \tag{3c}$$

By numerically solving eqn (3) (see the appendix), we obtain the concentration profiles as a function of time for all components of the system. We estimate magnitudes of the dimensionless parameters using parameters from the literature for phage T7 and related systems. The values for  $k_1$  and  $k_{-1}$  were measured for a phage T1-*E. coli* system in shaker culture (Garen, 1954). The viral diffusion constant  $D$  was measured for virus P22 (Stollar & Levine, 1963), which is similar in size and shape to T7. For the phage T7-*E. coli* system, the yield per infected host cell is around 200 for optimal conditions of exponentially growing hosts. However, this number could be much smaller in a growing plaque, where hosts are in

near stationary growth. In this study,  $Y$  has been arbitrarily set to 50 unless otherwise stated. Table 1 lists representative parameters applied in the simulations.

### Results

#### EXISTENCE OF A TRAVELING-WAVE SOLUTION

Concentration profiles for the virus and virus-host complex at different time points are shown in Fig. 1(a) and (b). We define the plaque radius,

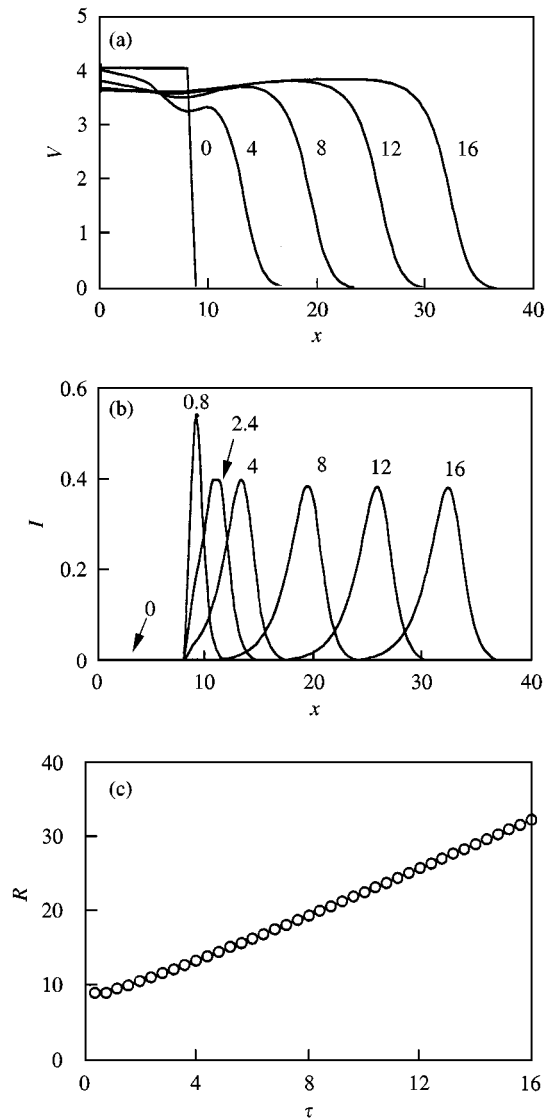


FIG. 1. Dimensionless concentration profiles of (a) virus and (b) virus-host complex at different dimensionless times, including early transient profiles. (c) Dimensionless plaque radius ( $R$ ) is plotted as a function of time ( $\tau$ ), indicating the existence of a traveling wave with a constant velocity. A yield ( $Y$ ) of 5 has been used for this simulation.

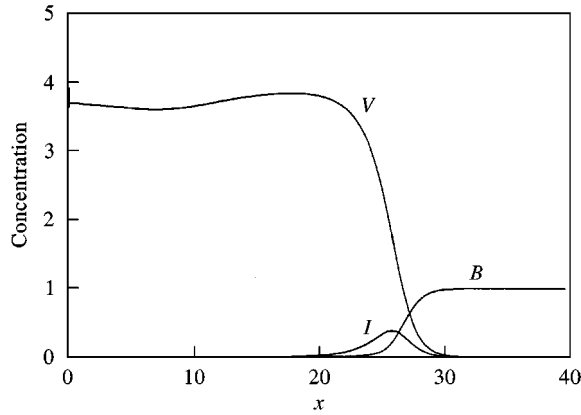


FIG. 2. Dimensionless concentration profiles for virus ( $V$ ), host ( $B$ ), and virus-host intermediate ( $I$ ) in the wave front of a growing plaque. The infection propagates to the right. In the laboratory a plaque is visible as a region where hosts have been lysed ( $B = 0$ ).

or distance traveled by the infection front, as the distance from the plaque center (at  $x = 0$ ) to the point where  $I$ , the dimensionless concentration of the virus-host complex, achieves its maximum. Plotting this radius against time, as in Fig. 1(c), gives a linear dependence, where the slope at any time is the front velocity. This result demonstrates the existence of constant-velocity traveling wave for this system, which was previously assumed but not shown (Yin & McCaskill, 1992). The propagation velocity is readily calculated by monitoring the radius change over a period where the plaque has moved beyond the transients associated with its initial conditions.

Concentration profiles within a well-established wavefront are shown in Fig. 2. The infection travels in the direction of increasing radius (ever larger  $x$ ), creating viruses ( $V$ ), through a virus-host intermediate ( $I$ ), at the expense of hosts ( $B$ ). Our model, when extended to allow for multi-virus adsorption to single hosts, finds negligible effects of multi-virus adsorption on the propagation velocity (data not shown). This result seems reasonable since the front velocity is determined by events at the leading edge of the front, where both  $I$  and  $V$  are too small to generate a significant population of multi-virus intermediates.

#### EFFECTS OF YIELD ( $Y$ ) AND ADSORPTION ( $\kappa_1$ ) ON THE PROPAGATION VELOCITY

An analytic solution that provides a relationship between the propagation velocity and the

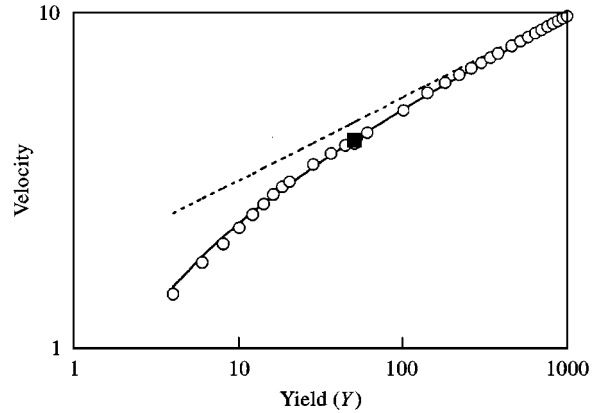


FIG. 3. Dependence of dimensionless propagation velocity on yield ( $Y$ ). The full analytic solution (—) agrees well with the simulation ( $\circ$ ). As expected, the explicit large- $Y$  analytical solution (---) converges with both solutions at large  $Y$ . The filled square is calculated from the representative parameters list in Table 1.

model parameters has been previously derived (Yin & McCaskill, 1992). That solution was based on a number of important assumptions: (1) a traveling wave solution exists for the system, (2) the host concentration at the leading edge of the front is much larger than virus and virus-host complex concentrations and can thus be treated as constant, (3) the shape of the concentration profile of each component approaches its limiting value as an exponential function, and all these exponential functions have the same decay length, and (4) the curvature of the plaque is negligible. As shown in Fig. 3, the full analytic solution matches well the results of our current simulation, indicating that the assumptions supporting the analytic solution were reasonable for capturing the velocity dependence on yield. The published large- $Y$  expression of velocity dependence on yield converges with the full solution at large yields, as expected.

The dependence of propagation velocity on  $\kappa_1$ , the dimensionless adsorption constant, is shown for the simulation and the analytic model in Fig. 4. The analytic model matches well the simulation for low and intermediate  $\kappa_1$ , but deviates at high  $\kappa_1$ , where the simulation asymptotically approaches its maximum. The discrepancy likely arises from the assumption for the analytic case that the exponential functions for all the species have the same decay length, which may well fail

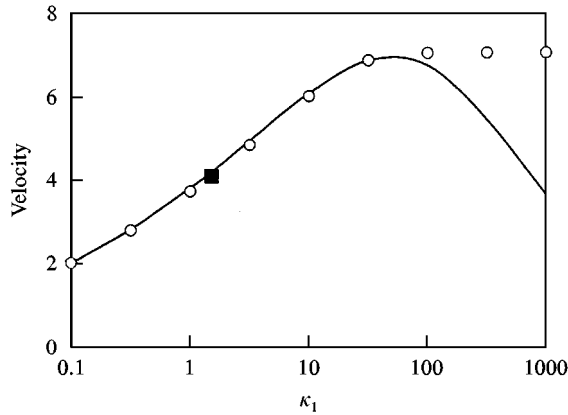


FIG. 4. Dependence of dimensionless propagation velocity on the dimensionless viral adsorption rate,  $\kappa_1$ . The simulated dimensionless propagation velocity ( $\circ$ ) approaches an asymptote as  $\kappa_1$  increases, while the analytic solution (—) breaks down as  $\kappa_1$  gets large. The filled square ( $\blacksquare$ ) is calculated from the representative parameters listed in Table 1.

for large  $\kappa_1$ . To develop an intuition for the large  $\kappa_1$  limit, consider the case of infinitely large  $\kappa_1$ , where viruses at the leading edge of the propagation front instantly adsorb to healthy host cells, form virus–host complexes, and in turn, produce more viruses. In this limit, the velocity of the infection is driven, as always, by the coupling of the autocatalytic virus amplification with the free viral diffusion, except that the amplification process loses the possibility for a kinetic bottleneck at the adsorption stage. Hence, as  $\kappa_1$  gets large, the velocity should become independent of  $\kappa_1$ , as we find in the simulation.

EFFECTS OF HINDERED DIFFUSION  
ON THE PROPAGATION VELOCITY

With the reaction–diffusion model in dimensionless form, the effect of host concentration on velocity is embedded in the effect of  $\kappa_1$  on velocity. Therefore, as shown above, the velocity will monotonically increase with increasing host concentration. This seems intuitively correct since host cells serve only as a resource for virus production. Higher host concentrations promote virus production and thus increase the propagation velocity. This result, however, is not consistent with experimental results where the velocity falls at high host concentrations. Host cells may also act as a barrier to viral diffusion. If we assume

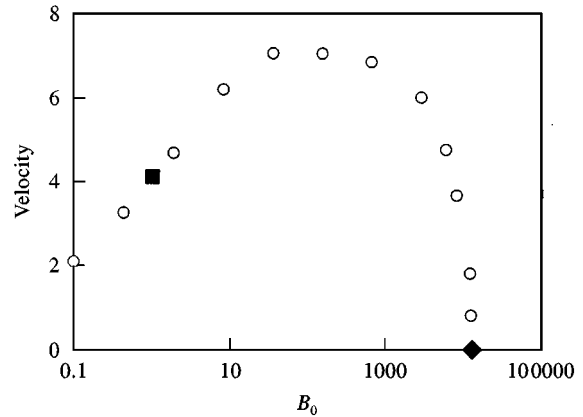


FIG. 5. Dependence of dimensionless propagation velocity on the host concentration, allowing for effects of hindered diffusion. At low host concentrations, increasing the host promotes production of viruses and faster propagation, but at high host concentrations the free virus diffusion is hindered, causing a drop in velocity. The filled square ( $\blacksquare$ ) is calculated from the representative parameters listed in Table 1, and the filled diamond is a virtual point when the entire space within the agar has initially been occupied by host cells. Since the effective viral diffusivity for this virtual situation is zero, the propagation velocity is also zero.

that host cells are impermeable spheres to viral diffusion until they are lysed, and the volume fraction occupied by host cells is  $\phi$ , we can approximate the effective viral diffusion constant as follows (Strieder & Aris, 1973; Cussler, 1984):

$$\frac{D_{eff}}{D} = \frac{2(1 - \phi)}{2 + \phi} \tag{4}$$

which gives the upper bound of the effective diffusivity for a given  $\phi$ . Assuming the volume of a host cell is  $V_h$ , we have  $\phi = V_h[B]$ , where  $[B]$  has units of number of cells per volume.  $D_{eff}$  is coupled with the instantaneous concentration of hosts, so it depends on time and position. However, since the propagation is driven by virus and host concentrations at the leading edge of the wavefront, where the host concentration is nearly constant,  $D_{eff}$  can still be treated as constant, as in the analytic model (Yin & McCaskill, 1992).

With the introduction of hindered diffusion, a biphasic effect of host concentration on propagation velocity arises, as shown in Fig. 5. When the host concentration is low, there is virtually no hindered effect from the hosts because of the low volume fraction they occupy. An increase in host

cell concentration initially contributes more to the production of new viruses than the hindering of diffusion, which overall increases the velocity. However, at high host concentrations, the balance shifts and hindered diffusion effects dominate, reducing the velocity.

#### EFFECTS OF LATENT TIME ON PROPAGATION VELOCITY

The kinetic parameter  $k_2$  is inversely proportional to the latent or generation time of an infection cycle. The propagation velocity equals  $(k_2 D)^{1/2}$  times the dimensionless propagation velocity. Hence, a change in  $k_2$  affects the overall propagation velocity in two ways—by changing the factor  $(k_2 D)^{1/2}$  and by changing the dimensionless velocity through the dimensionless parameters  $\kappa_1$  and  $\kappa_{-1}$ . As shown in Fig. 6 when  $k_2$  is small, the dimensionless propagation velocity can be represented as  $c = \alpha k_2^{1/2}$ , where the constant  $\alpha$  depends on other parameters of the system. The equation, as well as the plot, presents the dependence of propagation velocity on  $k_2$  in a form consistent with the earlier figures. This small  $k_2$  regime corresponds to the solution found by Koch (1964). However, as  $k_2$  increases, the dependence of propagation velocity deviates from this simple relationship.

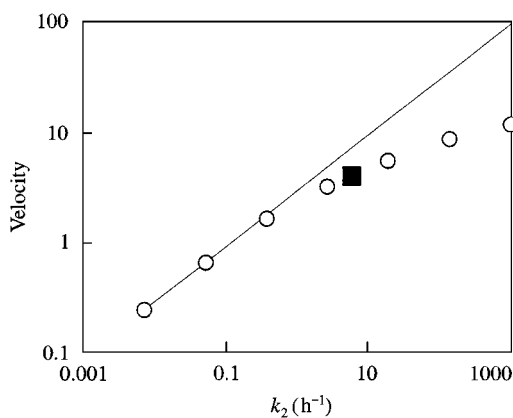


FIG. 6. Dependence of dimensionless propagation velocity on the production rate constant of new viruses,  $k_2$ . The dimensionless propagation velocity is proportional to the  $1/2$  power of  $k_2$  when  $k_2$  is small, a regime indicated by the solid line. The filled square (■) is calculated from the representative parameters listed in Table 1: (○) simulation; (—) small- $k_2$  asymptote.

## Discussion

Using the parameters in Table 1, we predict propagation velocities around  $1 \text{ mm h}^{-1}$ , about five-fold higher than experimentally observed (Yin & McCaskill, 1992). Here we consider how the model parameters would have to change to account for the high velocities obtained in simulations. For the phage T7 system,  $k_1$  and  $k_{-1}$  could be different from the values of Table 1, which are for a different phage. However, an unlikely change of several orders of magnitude in these parameters would be needed in order to account for the observed velocity. The diffusion constant  $D$  has been measured in agar for P22, a virus similar to in shape and size with phage T7, but it is unlikely that T7 will have a significantly different diffusion constant. Another important factor is the yield ( $Y$ ) of new virus particles per infected host cell. However, the dependence of velocity on yield is weak ( $c \propto Y^{1/4-1/2}$ ), indicating that a dramatic decrease in yield per host would be required to account for the small velocity, which again appears to be unlikely. Host concentration and latent time remain as potential factors to explain the discrepancy between simulated and measured velocities.

The process of plaque growth may be significantly influenced by the concurrent growth of the host. Experiments using a digital camera to mark the early stages of plaque and host-lawn growth show that initially, when the plaque is just distinct enough to be seen, the propagation velocity is usually at its maximum; it then falls to a slower constant value as the host-lawn approaches its growth limit (Lee & Yin, 1996b). Decreases in the initial velocity appear synchronous with the increase in host concentration (Lee & Yin, 1996b), supporting a dependence of propagation velocity on host concentration. By introducing the hindered effect of host cells on viral diffusion, the simulation shows a similar drop in propagation velocity when the host concentration is large (Fig. 5). Since none of the other parameters predict a similar relationship between the velocity and the host concentration, hindered diffusion appears to be important. However, a more subtle effect may be involved.

A reduction in the host growth rate decreases  $k_2$  by increasing the latent time, according to an

TABLE 1  
*Representative parameter values*

Parameter	Value	Dimensionless value	Notes and reference
$B_0$	$1 \times 10^8 \text{ ml}^{-1}$	1	
$V_h$	$8 \times 10^{-13} \text{ ml}$	$8 \times 10^{-5}$	Donachie & Robinson (1987)
$Y$	50	50	Yield is $\sim 200$ under optimal conditions
$k_1$	$9 \times 10^{-8} \text{ h}^{-1} \text{ ml}^{-1}$	1.5	Phage T1- <i>E. coli</i> (Garen, 1954)
$k_{-1}$	$3 \text{ h}^{-1}$	0.5	Phage T1- <i>E. coli</i> (Garen, 1954)
$D$	$1.44 \times 10^{-4} \text{ cm}^2 \text{ h}^{-1}$	1	Obtained for P22 (Stollar & Levine, 1963)
$k_2$	$6 \text{ h}^{-1}$	1	Estimated from the latent time of viral replication (Yin & McCaskill, 1992)

intracellular model for T7 growth (Endy, 1997). This prediction is qualitatively supported by our observation that a plaque cannot be *initiated* on host cells in stationary growth. Hence, the initial dependence of propagation velocity on host concentration could also be due to the decrease in  $k_2$  as the rate of host cell growth falls. This is also consistent with the observation that plaques initiated during rapid host growth can continue expanding 100 h (Yin, 1991), well beyond the transition to stationary-growth hosts. In this case, although the hosts far from the leading edge are in stationary stage, those right at the leading edge might resume growth since fragments of the dead cells could serve as nutrients.

Our numerical solution to the reaction-diffusion system provides a way to see how the rate of plaque growth can reflect the iterated dynamics of microscopic events at the level of single virus-host infections. We hope that this work may help us study the evolution of viruses in growing plaques. For example, our model could be extended to simulate evolutionary events by allowing for angular variation in species concentrations and introducing random perturbations in virus-host parameters during growth to simulate the effects of mutations. The development of spatial irregularities in the simulated plaque shapes could provide a means to interpret the magnitude of parameter changes needed to achieve the irregularities observed in evolving plaques in the laboratory (Yin, 1993; Lee & Yin, 1996a, b). Another possible extension of this model will be to couple it with a full intracellular viral growth model (Endy *et al.*, 1997; Endy, 1997). Such an extension could then bridge the macroscopically observable propagation velocity

directly with phage-host interactions at the genomic level.

### Conclusions

Our model provides a convenient means to explore the dynamics of the growing viral plaque by identifying how various factors can affect its radial propagation velocity. By relying on far fewer assumptions than our earlier analytic model, the numerical model here provides a means for testing the validity of our earlier assumptions. In particular, we demonstrate the existence of traveling-wave solution to the reaction-diffusion system and show the validity of the full analytic model for a broad range of yields and low to moderate adsorption-rate regimes. The small propagation velocity resulting from high host concentration, in turn, is probably due to the hindered effect of host cells on viral diffusion or an increase in latent time of the intracellular growth of virus, caused by the metabolic change in host cells.

We are grateful for support from the Whitaker Foundation and a National Science Foundation Presidential Early Career Award (PECASE) to J.Y. We would also like to thank W.E. Stewart for suggestions on the implementation of the numerical algorithm. Karen Duca and Drew Endy provided valuable comments and suggestions.

### REFERENCES

- ADAMS, M. (1959). *Bacteriophages*. New York: Interscience Publishers.
- CUSSLER, E. L. (1984). *Diffusion: Mass Transfer in Fluid Systems*. Cambridge: Cambridge University Press.
- DONACHIE, W. D. & ROBINSON, A. C. (1987). Cell division: parameter values and the process. In: *E. coli and S. typhimurium: Cellular and Molecular Biology*. (Neidhardt,

F. C., Ingraham, J. L., Low, K. B., Magasanik, B., Schaechter, M. & Umberger, H. E., (eds), pp. 1578–1593. Washington, DC: American Society for Microbiology.

ENDY, D. (1997). Development and application of a genetically-structured simulation for bacteriophage T7. Ph.D. Thesis. Dartmouth College.

ENDY, D., KONG, D. & YIN, J. (1997). Intracellular kinetics of a growing virus: a genetically structured simulation for bacteriophage T7. *Biotechnol. Bioeng.* **55**, 375–388.

GAREN, A. (1954). Thermodynamic and kinetic studies on the attachment of T1 bacteriophage to bacteria. *Biochim. Biophys. Acta* **14**.

KOCH, A. L. (1964). The growth of viral plaques during the enlargement phase. *J. theor. Biol.* **6**, 413–431.

LEE, Y. & YIN, J. (1996a). Detection of evolving viruses. *Nature Biotechnol.* **14**, 491–493.

LEE, Y. & YIN, J. (1996b). Imaging the propagation of viruses. *Biotechnol. Bioeng.* **52**, 438–442.

SAMBROOK, J., FRITSCH, E. F. & MANIATIS, T. (1989). *Molecular Cloning: a Laboratory Manual*. Cold Spring Harbor Laboratory Press.

STOLLAR, D. & LEVINE, L. (1963). Two-dimensional immunodiffusion. *Methods Enzymol.* **VI**, 848–854.

STRIEDER, W. & ARIS, R. (1973). *Variational Methods Applied to Problems of Diffusion and Reaction*. Berlin: Springer.

YIN, J. (1991). A quantifiable phenotype of viral propagation. *Biochem. Biophys. Res. Commun.* **174**, 1009–1014.

YIN, J. (1993). Evolution of bacteriophage T7 in a growing plaque. *J. Bact.* **175**, 1272–1277.

YIN, J. (1994). Spatially resolved evolution of viruses. *Ann. N. Y. Acad. Sci.* **745**, 399–408.

YIN, J. & MCCASKILL, J. S. (1992). Replication of viruses in a growing plaque: a reaction–diffusion model. *Biophys. J.* **61**, 1540–1549.

APPENDIX

Computational Details

In setting up the numerical scheme, we have taken advantage of the symmetry of the system by introducing a new coordinate  $\xi = x^2/4$ , which gives

$$\frac{\partial V}{\partial \tau} = g(\phi) \left( \xi \frac{\partial^2 V}{\partial \xi^2} + \frac{\partial V}{\partial \xi} \right) - \kappa_1 VB + (\kappa_{-1} + Y)I, \tag{A.1a}$$

$$\frac{\partial B}{\partial \tau} = -\kappa_1 VB + \kappa_{-1}I, \tag{A.1b}$$

$$\frac{\partial I}{\partial \tau} = \kappa_1 VB - (\kappa_{-1} + 1)I, \tag{A.1c}$$

with

BC:

$$V = 0, I = 0 \quad \text{as } \xi \rightarrow \infty,$$

$$\xi^{1/2}(\partial V/\partial \xi) = 0 \quad \text{at } \xi = 0 \text{ and } \xi \rightarrow \infty.$$

IC:

$$V = \begin{cases} V_0 & \text{for } \xi \leq \xi_0 \text{ at } \tau = 0, \\ 0 & \text{for } \xi > \xi_0 \text{ at } \tau = 0, \end{cases}$$

$$B = \begin{cases} 0 & \text{for } \xi \leq \xi_0 \text{ at } \tau = 0, \\ B_0 & \text{for } \xi > \xi_0 \text{ at } \tau = 0, \end{cases}$$

All the time derivatives are approximated using the forward difference

$$\frac{\partial X}{\partial \tau} \approx \frac{X_{i,j+1} - X_{i,j}}{\Delta \tau}, \tag{A.2a}$$

where  $X$  represents  $V, B$  or  $I$ .

The derivatives in  $\xi$  are approximated using the weighted averages of the finite differences at the  $j$ -th and the  $(j + 1)$ -th time point (the so-called implicit algorithm, shown to be more stable than the explicit algorithm, which makes use of only the derivative at the  $j$ -th time point):

$$\left[ \xi \frac{\partial V}{\partial \xi^2} + \frac{\partial V}{\partial \xi} \right] = \left\{ \lambda i \Delta \xi \left[ \frac{V_{i+1,j+1} - 2V_{i,j+1} + V_{i-1,j+1}}{(\Delta \xi)^2} \right] + (1 - \lambda) i \Delta \xi \left[ \frac{V_{i+1,j} - 2V_{i,j} + V_{i-1,j}}{(\Delta \xi)^2} \right] \right\} + \left\{ \lambda \frac{V_{i+1,j+1} - V_{i-1,j+1}}{2\Delta \xi} + (1 - \lambda) \frac{V_{i+1,j} - V_{i-1,j}}{2\Delta \xi} \right\}, \tag{A.2b}$$

